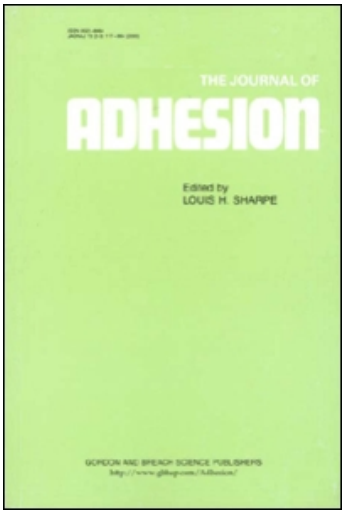

The Journal of Adhesion

Publication details, including instructions for authors and subscription information:
http://www.informaworld.com/smpp/title~content=t713453635

Recent Advances in the Application of Leaky Lamb Waves to the Nondestructive Evaluation of Adhesive Bonds

Cecil M. Teller[a]; K. Jerome Diercks[a]; Yoseph Bar-cohen[b]; Ajit K. Mal[c]
[a] Texas Research International, Inc., Austin, TX, U.S.A. [b] Douglas Aircraft Company, McDonnell Douglas Corporation, Long Beach, CA, U.S.A. [c] Mechanical, Aerospace and Nuclear Engineering Department, University of California, Los Angeles, CA, U.S.A.

To cite this Article Teller, Cecil M. , Diercks, K. Jerome , Bar-cohen, Yoseph and Mal, Ajit K.(1989) 'Recent Advances in the Application of Leaky Lamb Waves to the Nondestructive Evaluation of Adhesive Bonds', The Journal of Adhesion, 30: 1, 243 — 261
To link to this Article: DOI: 10.1080/00218468908048208
URL: http://dx.doi.org/10.1080/00218468908048208

J. Adhesion, 1989, Vol. 30, pp. 243–261
Reprints available directly from the publisher
Photocopying permitted by license only

Printed in the United Kingdom

Recent Advances in the Application of Leaky Lamb Waves to the Nondestructive Evaluation of Adhesive Bonds†

CECIL M. TELLER and K. JEROME DIERCKS

Texas Research International, Inc., 9063 Bee Caves Road, Austin, TX 78733-6201, U.S.A.

YOSEPH BAR-COHEN

Douglas Aircraft Company, McDonnell Douglas Corporation, Long Beach, CA 90846-0001, U.S.A.

AJIT K. MAL

Mechanical, Aerospace and Nuclear Engineering Department, University of California, Los Angeles, CA 90024-1597, U.S.A.

(Received October 21, 1988; in final form July 19, 1989)

In earlier work, the feasibility of applying the Leaky Lamb Wave (LLW) method to the nondestructive evaluation (NDE) of bonded rubber/metal structures was demonstrated. The capability of LLWs to detect and delineate flaws at the bond line was proven, even when the adherends remain in intimate contact. However, variations in adherend properties, surface orientation and thickness can adversely affect detection of bond flaws and assessment of bond quality. In this paper, parameters which degrade both LLW sensitivity and resolution to bond flaws are discussed. Examples of the effects of cold work, thickness change and specimen tilt are presented along with bond flaw detection and characterization results. Also, advances in the theory of bond flaw NDE by LLWs are presented.

KEY WORDS NDE of adhesive bonds; application of Leaky Lamb Waves to NDE of adhesive bonds; wave propagation theory; rubber to metal adhesive bonds; effects of adherend properties on Leaky Lamb Wave sensitivity and resolution; adhesive bond quality measurements.

1 INTRODUCTION

Adhesives have many potential advantages over conventional fasteners (bolts, rivets, etc.) for accomplishing efficient load transfer. One of the most important advantages is that stresses are distributed over larger areas. For example, in aerospace structures the possibility of fatigue failure due to stress concentrations can be significantly reduced using adhesive bonds instead of mechanical fasteners.

† Presented at the 35th Sagamore Army Materials Research Conference, Manchester, New Hampshire, U.S.A., June 26–30, 1988.
© Chemlok is a registered trademark of the Lord Corporation, Chemical Products Group.

Adhesives are also used to join dissimilar materials not easily joined by other means. For example, rubber/metal bonds of importance to watertight integrity of marine structures such as sonar transducers are made using vulcanizing adhesives.

Although adhesives have been in use for joining aerospace and marine structures for many years, they have not generally lived up to the reliability requirements placed on these structures. One important reason is that adequate nondestructive evaluation (NDE) methods of inspecting bonded structures are not presently available. Thus, the challenge to the NDE community is to develop new inspection methods which can be used to evaluate the quality and integrity of bonded joints. This challenge is the motivation for the present work with the Leaky Lamb Wave (LLW) method.

The LLW and other similar ultrasonic methods have been shown to be promising NDE tools for detecting and characterizing various defects in composites and adhesively bonded joints.[1-4] In prior work by the authors, the LLW method was shown to be capable of detecting and delineating bondline flaws in rubber/metal laminates, even when the adherends remain in intimate contact.[1-2]

Although promising, the LLW method is affected by conditions other than the presence of bondline flaws such as variations in adherend properties, surface condition and surface geometry. An insufficient understanding of the LLW phenomenon and the complexity of the associated acoustic field has hampered progress in the application of LLW to composites and bonded joints. Thus, the LLW method is a new approach to inspecting bonded structures including composites, metals and dissimilar materials, which deserves further research.

This paper presents a status report on the application of the LLW method to the NDE of adhesive bonds between rubber and steel adherends. Advances in both the theory and the experimental research to understand the influence of the metal adherend properties of the LLW signals are discussed. Recent results on detecting and characterizing bond line flaws are also covered.

2 PROGRESS ON THE THEORY

A schematic description of the LLW experiment is shown in Figure 1. A pair of broadband transducers is placed in a coupling fluid (usually water) in a

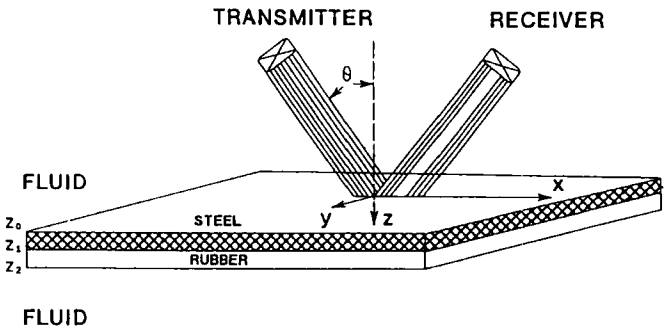

FIGURE 1 Schematic of the leak Lamb wave field for a steel/rubber bond.

pitch-catch arrangement, and the specimen, immersed in the fluid, is insonified by a beam of acoustic waves. For a given incidence angle, guided Lamb-type waves are induced in the specimen at certain specific frequencies of excitation, resulting in leakage of energy into the fluid and the occurrence of a null or minimum in the reflected field. The phase velocity of the guided waves, v, is related to the incident angle, θ, through Snell's law,

$$v = v_0/\sin\theta \tag{1}$$

where v_0 is the acoustic wave speed in water. Further, when leaky waves are present, the amplitude spectrum of the reflected wave shows prominent minima at a number of frequencies, $f_1, f_2, f_3, \ldots, f_n$, at which the velocity of the guided waves of different modes in the specimen is v. For a given angle of incidence, θ, or equivalently from (1), the phase velocity, v, the frequencies of the leaky guided wave modes can be determined by sweeping through a given frequency range and searching for minima in the reflected amplitude at the null location. By changing the angle of incidence, the phase velocity-frequency relation, or the so-called *dispersion curves* of leaky guided waves in the specimen can thus be measured with considerable accuracy by means of the LLW technique.[5]

The usefulness of the LLW technique stems from the fact that both the speed and amplitude of the guided waves in the plate are strongly dependent upon the material, interface and other properties of the specimen. Thus, it should, in principle, be possible to estimate some of these properties through inversion of the LLW data. However, development of reliable inversion schemes requires the availability of a theoretical model containing the essential features of the wave phenomena associated with the experiment. As indicated in the Introduction, such theories are in their formative stages at present, and much research is needed before they can be used in realistic situations. We present a brief description of a theory based on a highly idealistic model which has, nevertheless, been found to give results that agree quite well with LLW data for a variety of specimens. The details of this theory and references to other related work can be found in Mal[6] and Bar-Cohen and Mal.[7]

In the present Steel/Rubber bond problem, we assume that

1) Both steel and rubber are elastic and isotropic.
2) The interface is either perfectly bonded or completely unbonded.
3) The incident beam is a plane wave.

The first assumption appears to be approximately correct for the specimens tested by us. The second assumption is for convenience at this stage of the theoretical development; in future work partial bonding and interfacial features will be considered based on the theory developed in Mal.[6] The last assumption has been shown to work very well in the frequency range of interest. The main objective of the theory is to calculate the reflection and, if needed, the transmission coefficients as functions of frequency and incident angle.

The geometry of the bonded plate containing N-2 interfaces and two free surfaces and immersed in water is shown in Figure 1 together with a coordinate

system (x, y, z). The material properties of the mth layer bounded by $z = z_{m-1}$ and $z = z_m$ are denoted by $h(m)$(thickness), $\rho(m)$(density), $c_1(m)$(longitudinal wave speed) and $c_2(m)$(transverse wave speed). The wave numbers of the longitudinal and transverse waves in the mth layer, $k_1(m)$ and $k_2(m)$ are defined as,

$$k_\alpha(m) = \omega/c_\alpha(m), \qquad \alpha = 1, 2$$

where ω is the circular frequency. The relevant displacement and stress components at any point in the plate due to the excitation by an incident plane wave, assumed to be independent of y, are denoted by

$$\begin{Bmatrix} u(x, z) \\ w(x, z) \end{Bmatrix} = \{U(z)\} e^{ikx - i\omega t} \tag{2a}$$

$$\begin{Bmatrix} \tau_{xz}(x, z) \\ \sigma_z(x, z) \end{Bmatrix} = \{T(z)\} e^{ikx - i\omega t} \tag{2b}$$

where $\{U\}$, $\{T\}$ are the z-dependent parts of the displacement and stress vectors defined in (2) and $k = (\omega/v_0) \sin \theta$.

Let the vectors $\{U\}$ and $\{T\}$ be assembled into a four-dimensional vector $\{S(z)\}$, called the displacement-stress vector $\{S(z)\}$ in the mth layer as

$$\{S(z)\} = \begin{Bmatrix} U \\ T \end{Bmatrix}. \tag{3}$$

The unknown vector $\{S(z)\}$ needs to be determined through substitution of the assumed form (2) of the displacement and stress components in Cauchy's equation of motion, namely,

$$\sigma_{ij,j} + \rho\omega^2 u_i = 0 \tag{4}$$

where standard index notation has been used. The result is that $\{S(z)\}$ is expressible in the partitioned form as

$$\{S(z)\} = \begin{bmatrix} Q_a(m) & Q_b(m) \\ Q_c(m) & Q_d(m) \end{bmatrix} [E(z, m)] \begin{Bmatrix} C^+(m) \\ C^-(m) \end{Bmatrix} \tag{5}$$

for $z_{m-1} < z < z_m$. In (5) $\{C^+(m)\}$ and $\{C^-(m)\}$ are unknown, two-dimensional constant vectors corresponding to the downgoing and upgoing waves, respectively, $[E(z, m)]$ is the diagonal matrix defined as,

$$[E(z, m)] = \text{diag}[e_1(z - z_{m-1})\, e_2(z - z_{m-1})\, e_1(z_m - z)\, e_2(z_m - z)] \tag{6}$$

and the submatrices in (5) are given by

$$[Q_a(m)] = \begin{bmatrix} ik & \eta_2 \\ -\eta_1 & ik \end{bmatrix} \qquad [Q_b(m)] = \begin{bmatrix} ik & -\eta_2 \\ \eta_1 & ik \end{bmatrix} \tag{7a}$$

$$[Q_c(m)] = \begin{bmatrix} -2ik\eta_1\mu & \zeta\mu \\ \zeta\mu & -2ik\eta_2\mu \end{bmatrix} \qquad [Q_d(m)] = \begin{bmatrix} 2ik\eta_1\mu & -\zeta\mu \\ \zeta\mu & 2ik\eta_2\mu \end{bmatrix} \tag{7b}$$

where

$$\zeta(m) = k^2 + \eta_2^2(m) \tag{7c}$$

$$e_\alpha(z) = e^{-\eta\alpha^{(m)}z} \tag{7d}$$

$$\eta_\alpha(m) = [k^2 - k_\alpha^2(m)]^{1/2}, \quad Im[\eta_\alpha(m)] < 0 \tag{7e}$$

where "Im" indicates the imaginary part of a complex quantity.

The constant vectors $\{C^+(m)\}$ and $\{C^-(m)\}$ must be determined from the interface and boundary conditions. For perfect bonding, the vector $\{S(z)\}$ is continuous across the interface, $z = z_m$, and this can be expressed as

$$\begin{bmatrix} Q_a(m+1) & Q_b(m+1)E(m+1) \\ Q_c(m+1) & Q_d(m+1)(E(m+1) \end{bmatrix} \begin{Bmatrix} C^+(m+1) \\ C^-(m+1) \end{Bmatrix} - \begin{bmatrix} Q_a(m)E(m) & Q_b(m) \\ Q_c(m)E(m) & Q_d(m) \end{bmatrix} \begin{Bmatrix} C^+(m) \\ C^-(m) \end{Bmatrix} = 0 \tag{8a}$$

where $[E(m)]$ is the diagonal matrix,

$$[E(m)] = \text{diag}[e^{-\eta_1(m)h(m)}\, e^{-\eta_2(m)h(m)}]. \tag{8b}$$

For a layered plate immersed in a fluid and subjected to obliquely-incident plane waves, the boundary conditions at the top ($z = 0$) and bottom ($z = H$) surfaces are given by

$$\{S(0)\} = \{U_0 \;\; i\eta_0(1-R) \;\; 0 \;\; -\rho_0\omega^2(1+R)\} \tag{9a}$$

$$\{S(H)\} = \{U_N \;\; i\eta_N T \;\; 0 \;\; -\rho_N\omega^2 T\} \tag{9b}$$

where R and T are the reflection and transmission coefficients, and the fluid properties at the top and bottom are denoted by the subscripts 0 and N, respectively.

Equations (8) and (9) provide $4N$ equations for the $4N$ unknowns, namely, $\{C^\pm(m)\}$, $m = 1, 2, \ldots, N-1$, U_0, U_N, R and T, and they can be solved for all the unknowns including the reflection coefficient, R, which is of primary interest here.

For the two-layered plate immersed in water shown in Figure 1, the linear system can be written explicitly as

$$[Q]\{C\} = \{B\} \tag{10a}$$

where

$$\{C\} = \{C^-(0) \;\; C^+(1) \;\; C^-(1) \;\; C^+(2) \;\; C^-(2) \;\; C^+(3)\} \tag{10b}$$

$$\{C^-(0)\} = \{U_0 R\}, \quad \{C^+(3)\} = \{U_3 T\} \tag{10c}$$

$$\{B\} = \{0 \;\; i\eta_0 \;\; 0 \;\; -\rho_3\omega^2 \;\; 0 \;\; 0 \;\; 0 \;\; 0 \;\; 0 \;\; 0 \;\; 0\} \tag{10d}$$

where $\rho_0 = \rho_3$ is the density of water. In (10), the matrix $[Q]$ has been assembled

in the global form,

$$\begin{bmatrix} -Q_b(0) & Q_a(1) & Q_b(1)E(1) & 0 & 0 & 0 \\ -Q_d(0) & Q_c(1) & Q_d(1)E(1) & 0 & 0 & 0 \\ 0 & -Q_a(1)E(1) & -Q_b(1) & Q_a(2) & Q_b(2)E(2) & 0 \\ 0 & -Q_c(1)E(1) & -Q_d(1) & Q_c(2) & Q_d(2)E(2) & 0 \\ 0 & 0 & 0 & -Q_a(2)E(2) & -Q_b(2) & Q_a(3) \\ 0 & 0 & 0 & -Q_c(2)E(2) & -Q_d(2) & Q_c(3) \end{bmatrix} \tag{11a}$$

In (11a), the submatrices with arguments 1 and 2 are defined in (7), while the remaining ones are given by,

$$[Q_b(0)] = \begin{bmatrix} 1 & 0 \\ 0 & -i\eta_0 \end{bmatrix}, \quad [Q_d(0)] = \begin{bmatrix} 0 & 0 \\ 0 & -\rho_0\omega^2 \end{bmatrix}, \tag{11b}$$

$$[Q_a(3)] = \begin{bmatrix} 1 & 0 \\ 0 & i\eta_0 \end{bmatrix}, \quad [Q_c(3)] = \begin{bmatrix} 0 & 0 \\ 0 & -\rho_0\omega^2 \end{bmatrix}. \tag{11c}$$

The reflection coefficient, R, can be calculated by solving the linear system (10). For guided waves propagating in the layered medium in absence of fluid, the dispersion equation is

$$F(k,f) = \begin{vmatrix} -Q_c(1) & Q_d(1)E(1) & 0 & 0 \\ -Q_a(1)E(1) & -Q_b(1) & Q_a(2) & Q_b(2)E(2) \\ -Q_c(1)E(1) & -Q_d(1) & Q_c(2) & Q_d(2)E(2) \\ 0 & 0 & -Q_c(2)E(2) & -Q_d(2) \end{vmatrix} = 0 \tag{12}$$

which has been obtained by eliminating certain rows and columns of the global matrix $[Q]$ in (11). The solution of this equation gives the phase velocity of the guided waves, $v = \omega/k$, as a function of frequency. We have developed computer codes based on the global matrix formulation to calculate the reflection coefficient from (10) and the dispersion curves from (12) without encountering the well-known numerical instability at higher frequencies.

A typical result of theoretical calculations is presented in Figure 2. The models used in the calculations include (a) bare steel plate of 1/4″ (6.35 mm) thickness and (b) the same steel plate with a 1/8″ (3.18 mm) rubber backing with perfect bond. The material properties used in the calculations are given in Table I. The amplitude spectra, as well as the time history of the reflected waves for a 25° incident angle, are shown in Figure 2. It can be seen that the two cases, namely, bare steel and steel/rubber, give only slightly different results for the spectral amplitudes and time histories. This was found to be true for all other angles of incidence and at other frequency ranges. There is, however, one feature of the reflected amplitude spectra that is significantly different in the two cases, namely the depth of the minima. The location and depth of the first spectral minimum for the two models are listed in Table II for a range of angles. This difference is the basis for the interpretation of LLW data as explained in the Appendix.

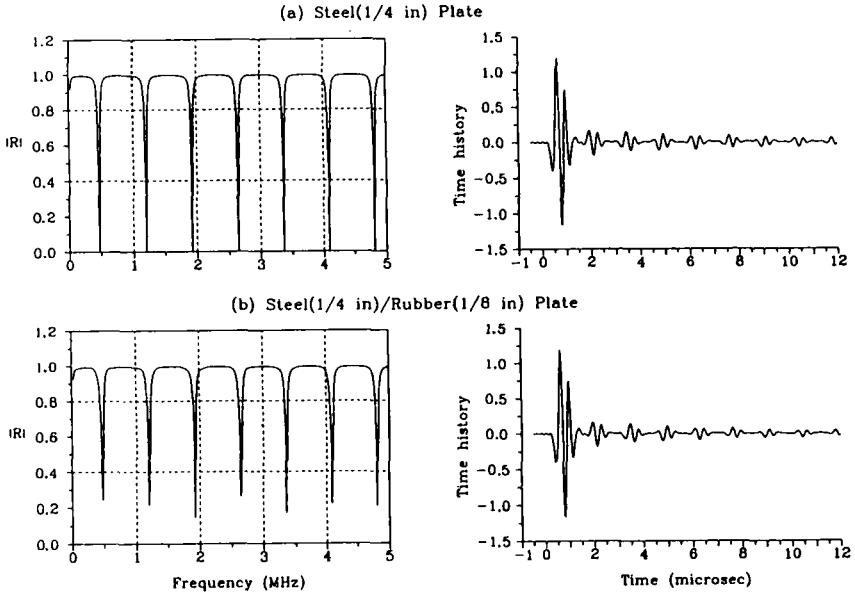

FIGURE 2 LLW spectra (left) and time histories (right) for a bare steel plate and two models of steel/rubber bond. Incident angle is 25° and the incident pulse has 2.5 MHz center frequency.

TABLE I
Material properties used in theory

	Thickness (mm)	ρ (g/cc)	α (mm/μsec)	β (mm/μsec)
Steel	6.35	7.86	5.99	3.31
Rubber	3.175	1.45	1.58	0.24

TABLE II
Amplitudes of minimum reflection coefficients

Incidence angle (degrees)	Frequency (MHz)	Amplitude of R	
		Bare steel (1/4")	Steel (1/4")/ rubber (1/8")
15	0.565	0	0.4008
17	0.315	0	0.0986
20	0.390	0	0.3534
25	0.474	0	0.2921
38	0.619	0	0.2070

3 EXPERIMENTAL RESULTS AND DISCUSSION

Experiments were conducted to investigate the LLW response of steel plate specimens, with and without bonded rubber layers. (See Table III for a description of the specimens and the Appendix for details of the experimental procedures.) In these experiments, changes in the metallurgical condition, specimen orientation and thickness of the plate were of interest. Experiments were also conducted to determine the LLW response of a special strip debond specimen. In each case only representative results are reported.

3.1 Metallurgical condition (stainless steel adherend)

Specimens 1 and 2 were taken from adjacent positions in a large Type 304 stainless steel plate. The large plate had been cold-rolled (40% reduction in area), annealed, pickled and tempered to produce a yield strength of 45,500 ksi. Thus, both specimens originally had the same degree of cold work, rolling texture (grain size and orientation) and hardness. The difference between the two is that Specimen 2 was further annealed for 12 hr at 1850°F. This annealing produced an increase in ASTM E112 grain size from 6 to 3, about a factor of 8. Also, the hardness was reduced from R_B86 to R_B75.

TABLE III
Specimens

Specimen no.	Material	Thickness (in.)	Comments
1	Type 304 Stainless Steel Cold-Rolled Annealed, Pickled and Tempered	0.250	Used as Received
2	Type 304 Stainless Steel Cold-Rolled Annealed, Pickled and Tempered	0.250	Annealed Before Use. Heated to 1850°F, Then Forced-Air Cooled
3	Type 304 Stainless Steel Cold-Rolled Annealed, Pickled and Tempered	0.250	Used as Received
4	AISI 1018 Carbon Steel Cold-Drawn	0.240	Used as Received. Steps Machined in Surface Parallel to Drawing Direction.
5	AISI 1018 Carbon Steel Cold-Drawn	0.240	Used as Received. Rubber bonded over 2/3 the lower surface area.

Figures 3 and 4 are LLW waterfall scans of Specimens 1 and 2, respectively. (See the Appendix for a description of the LLW display formats.) Three scans are shown in each of the figures for three different orientations of the transducers. A "normal" scan is one with the plane of the transmitter/receiver pair (wave propagation direction) oriented orthogonal to the scanning direction and parallel to the rolling direction of the specimens. The ±45° orientations mean that the transducer pair was rotated about the vertical axis to these respective angles to make the scan. Rotation was done to investigate the effects of grain scattering.

Several differences are evident in Figures 3 and 4. First, the overall signal level of Specimen 2 is much lower than that of Specimen 1, and second, the character of the signal is changed significantly by the annealing. In addition, the three transducer orientations (with respect to the rolling direction) produce three different results in the Specimen 1 scans, whereas those of Specimen 2 are essentially the same indicating the more uniform response from this specimen for the three directions tested. The prominent feature near the right side of Figure 3 is due to a surface indentation (heavily cold-worked area observed in a micrograph) in Specimen 1 not present in Specimen 2. The high level signal near the top is due to parallel grooves about 0.004–0.006 in. deep on the surface of Specimen 1 along its top edge believed to be caused by clamping the large plate during levelling and cutting operations.

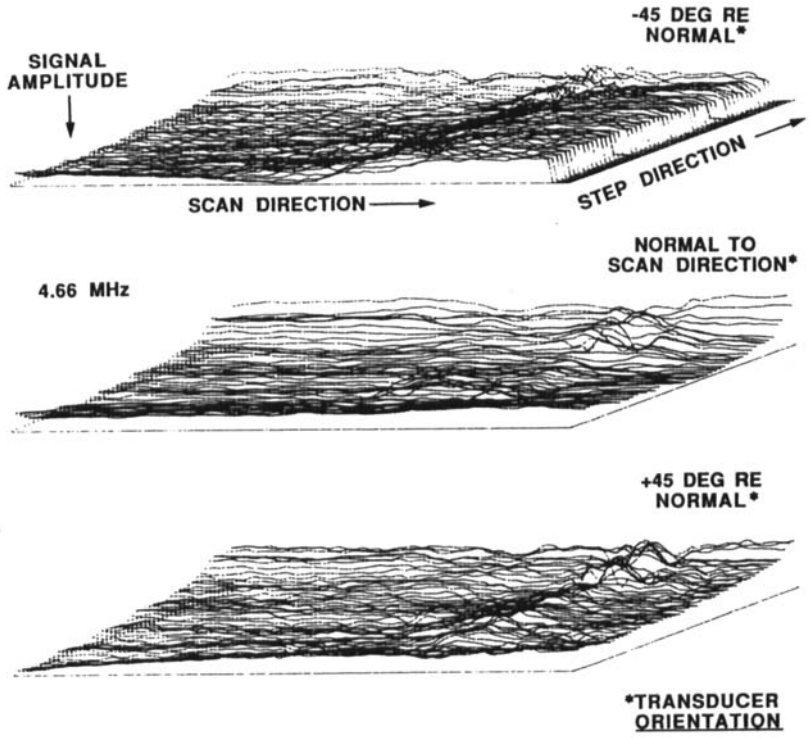

FIGURE 3 Leaky Lamb wave waterfall scans of specimen 1 showing the effects of cold work.

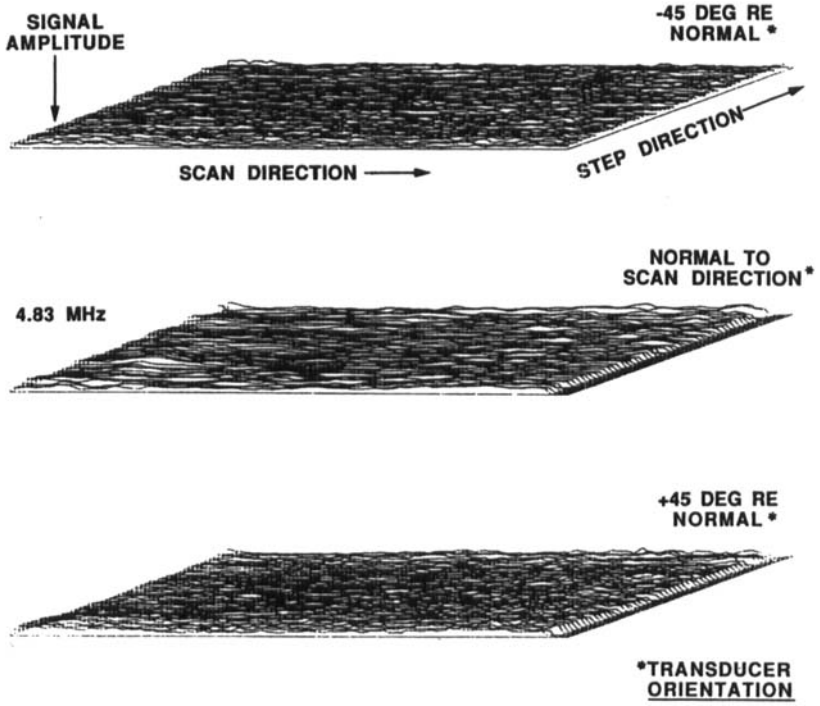

FIGURE 4 Leaky Lamb wave waterfall scans of specimen 2 showing the effects of annealing.

The interpretation of these results is as follows. Specimen 1 scans are mostly influenced by the presence of cold work as evidenced by the high level signals from the indentation and the grooves. The general microstructure shows small grains that are not highly oriented along the rolling direction, so the changing character of the LLW signal with transducer orientation was not significantly influenced by grain orientation and scattering. In Specimen 2 the directionality of the LLW response is minimal although scattering from the larger grains is contributing to the overall lower signal level (i.e., attentuation of the signal in the pitch-catch transducer arrangement). Also, the hardness of this specimen was significantly reduced by the annealing, indicating further relief of the effects of cold working. Most interesting is the fact that the high-level signal from the surface grooves has disappeared in the Specimen 2 scans even though the grooves are, of course, still physically present after annealing. This suggests that the signal from the grooves in Specimen 1 was due to the localized deformation and associated residual stresses present in the as-received material but removed by additional annealing.

3.2 Plate orientation and thickness

To investigate the effects of plate orientation on the LLW response, Specimen 3 (Type 304 stainless steel) was scanned in the as-received condition with its surface

parallel to the scan plane to within a fraction of a wavelength of the signal frequency. The specimen was then tilted about one wavelength (0.029 in.) left to right and scanned again.

As shown in the LLW color C-scans of Figure 5, there is a significant change in the relatively high background response due to the tilt of this constant thickness plate. The striations at the top of each figure are due to surface grooves in the plate during cold rolling as discussed previously. They are, in effect, surface roughness which can yield a high-level background signal if the effects of deformation (cold work and residual stresses) are present.

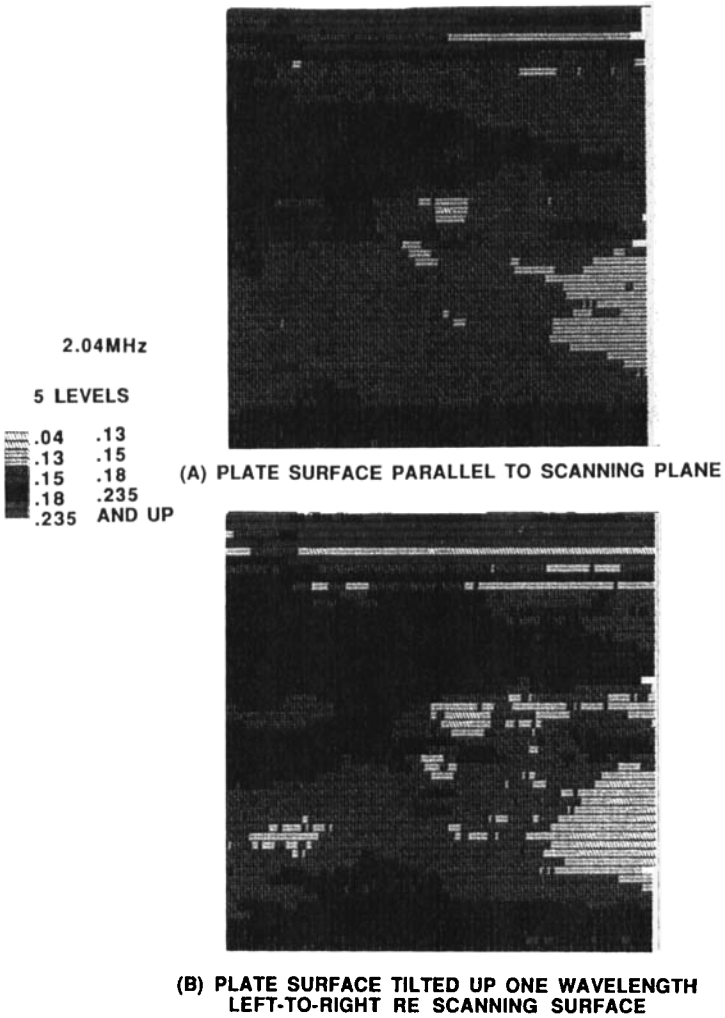

FIGURE 5 Leaky Lamb wave color C-scans of specimen 3 showing the effects of specimen orientation (tilt). See color plate I.

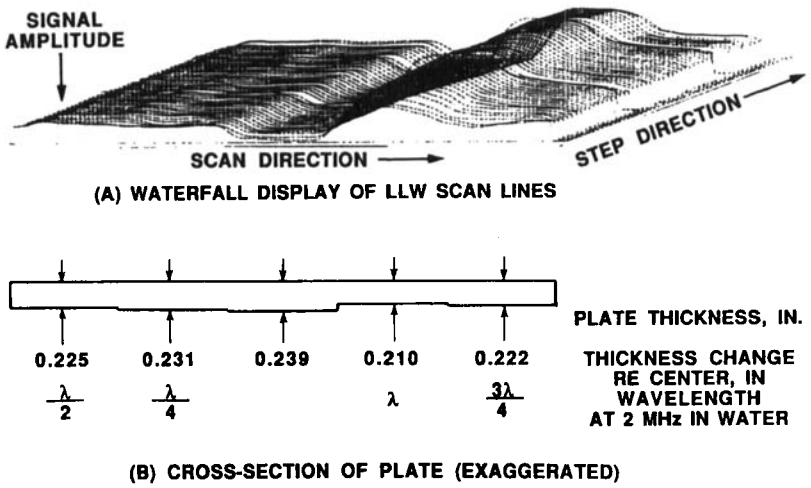

FIGURE 6 Leaky Lamb wave waterfall scan and cross-sectional view of specimen 4 showing the effects of thickness change.

Figures 6 and 7 show the effect of varying plate thickness on the LLW signal using two display formats. Figure 6(b) is a diagram of Specimen 4 (AI5I 1018 steel) that has steps machined in one surface of the depths indicated. Note that the waterfall display of Figure 6(a) emulates the change in plate thickness and that there is a rather large difference in signal level going from the center position (full plate thickness of 0.239 in.) to the deepest step immediately to the right

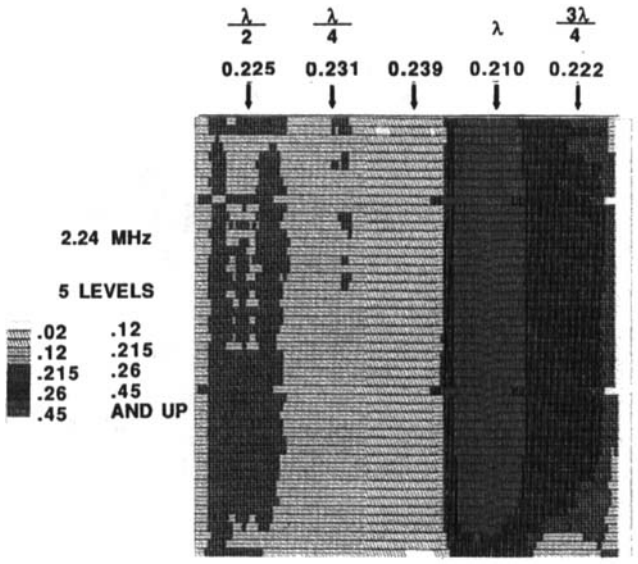

FIGURE 7 Leaky Lamb wave color C-scan of specimen 4 showing the effects of thickness change. See color plate II.

(plate thickness of 0.210 in.). This change in thickness is equivalent to one wavelength (0.029 in.) at the signal frequency. In Figure 7 the steps show up clearly in the C-scan image as a significant shift in signal level going from one step to the next.

The results obtained from Specimens 3 and 4 suggest that simply tilting a constant-thickness plate on the order of one wavelength has a measurable effect on the LLW background signal. Also, varying plate thickness in small steps up to one wavelength has an even greater effect.

3.3 Bond flaw detection

Figure 8 is a diagram of Specimen 5 (AISI 1018 steel), a specially prepared rubber/steel specimen with an intentional defect. The approximately 0.5 in. wide strip debond shown to the right of the center was formed as discussed in the Appendix. Subsequently, a 0.12 in. neoprene rubber layer was bonded over approximately two-thirds of the prepared surface as shown in the figure. After the specimen was cured, a thin spatula was inserted from the top to open the strip debond for a distance of about half its length.

Figure 9 shows an LLW color C-scan of Specimen 5 that clearly indicates the presence of the strip debond at the rubber-steel interface (steel side facing the transducers). Also note the difference in signal level between the region of the debond that was opened with the spatula and the region that was not opened. The difference between these two regions is that the surfaces remain in tight

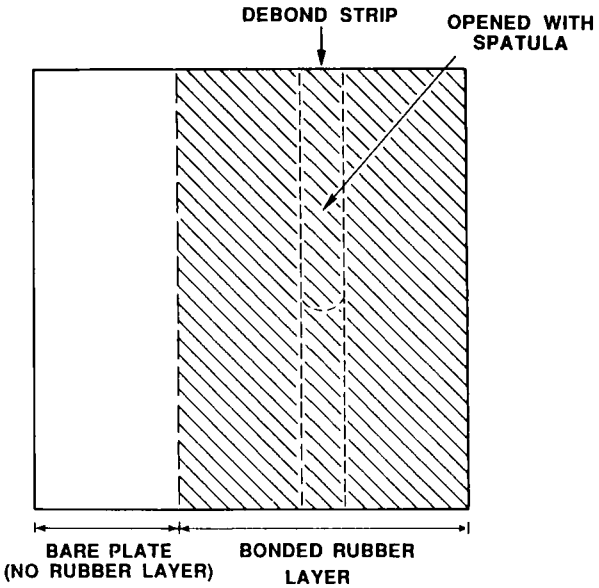

FIGURE 8 Plan view of specimen 5, a bonded AISI 1018 steel and 5109S neoprene rubber laminate with an intentional debond.

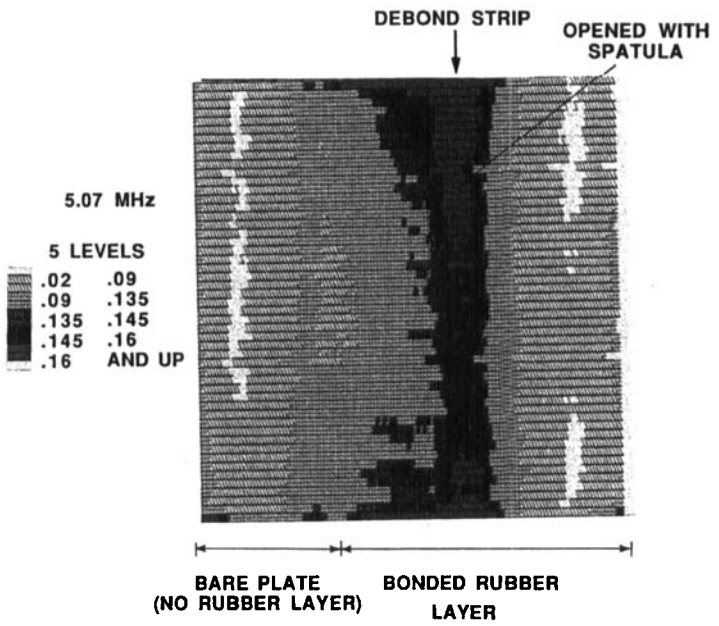

FIGURE 9 Leaky Lamb wave color C-scan of specimen 5 showing the variation in response between tight and opened areas of the debond. See color plate III.

contact from the pressure bonding (vulcanizing) process in the region where they were not separated by the spatula. This ability to distinguish between a "disbond" in which the surfaces are in tight contact and an "unbond" in which the surfaces have been separated and then allowed to relax to kissing contact is considered to be a prime advantage of the LLW method over conventional bond inspection methods. It should be noted that the widening of the debond at the top and bottom edges of Specimen 5 is a real effect, i.e., the debond actually was spread out at the edges as noted during close visual examination after the C-scan image was obtained.

4 CONCLUDING REMARKS

It is apparent from this work that the LLW method is a very promising method of adhesive bond inspection. However, much still needs to be understood about the way in which the propagating wave interacts with the metallic adherend so that interpretation of the flaw response can be made more certain.

From the experimental work, the chief contributor to the background signal in the as-received stainless steel specimens appears to be the degree of cold work and localized residual stress associated with plastic deformation. Annealing produced a more uniform LLW response, even though there was more attenuation of the signal in the large grain specimen. Variations in orientation and thickness of the metallic adherend also cause a significant shift in background

level. However, for a constant thickness metallic adherend moderate tilt can be accommodated by maintaining a constant spacing (lift-off) between the transducers and the specimen.

In terms of flaw detection the LLW method is sensitive not only to the presence of debonds at the metal/rubber interface, but also to the degree of openness of the debond. However, to be effective in discriminating bond flaws in engineering materials of practical importance (forgings, castings, machined parts), there needs to be a way to interpret the LLW signal from the flaw in the presence of confounding influences due to variations in the metallic adherend properties and thickness.

Acknowledgment

Support for this work was provided by the Office of Naval Research, Small Business Innovative Research Program, Dr. L. H. Peebles, Scientific Officer.

References

1. C. M. Teller, K. J. Diercks, Y. Bar-Cohen and N. Shah, "Nondestructive Evaluation of Adhesive Bonds," presented at 16th Symposium on Non-destructive Evaluation, Sponsored by NTIAC, San Antonio, TX, April 21–23, 1987.
2. C. M. Teller, K. J. Diercks, Y. Bar-Cohen and N. N. Shaw, "Nondestructive Evaluation of Adhesive Bonds," in *Review of Progress in Quantitative Nondestructive Evaluation*, D. O. Thompson and D. E. Chimenti, Eds. (Plenum Press, New York, 1988) Vol. 7B, pp. 935.
3. A. Pilarski and J. L. Rose, "A Transverse Wave Ultrasonic Oblique Incidence Technique for Internal Weakness Detection in Adhesive Bonds," *J. Appl. Phys.* **63,** 300–307 (1988).
4. S. Rokhlin and D. Marom, "Study of Adhesive Bonds Using Low-Frequency Obliquely Incident Ultrasonic Waves," *J. Acoustic. Soc. Am.* **8,** 245–258 (1986).
5. Y. Bar-Cohen, "Ultrasonic NDE of Composites—A Review," in *Solid Mechanics Research for Quantitative NDE,* J. D. Achenbach, and Y. Rajapakse, Eds. (Marinus Nijhoff Publishers, Boston, 1987), pp. 197–201.
6. A. K. Mal, "Guided Waves in Layered Solids with Interface Zones," *Intern. J. Engr. Sci.* **26,** 873–881 (1988).
7. Y. Bar-Cohen and A. K. Mal, "Ultrasonic NDE of Adhesive Bonding," sub-section of Section 14 (Applications), *ASNT Handbook, Vol. 6: Ultrasonic Testing,* R. Green, Jr., Ed (forthcoming).

APPENDIX

EXPERIMENTAL PROCEDURES

This Appendix describes in detail the experimental procedures used to obtain Leaky Lamb Wave data. It covers specimen preparation, instrumentation, set-up conditions and measurement procedures.

Specimen preparation

Bare steel specimens were prepared from 0.25 in. thick plates of Type 304 stainless steel and AISI 1018 carbon steel. Specimen size was 6 × 6 in. Most of the

bare metal plates were buffed with 400 grit sandpaper followed by vapor degreasing for 30 min. Some of the plates were examined in the as-received condition.

Bonded rubber-to-metal specimens were prepared according to the following procedure. The steel plates were vapor degreased and the bonding surfaces grit blasted with No. 50 grade coarse grit. After grit blasting the plates were cleaned with MEK and vapor degreased again for 30 min. The plates were allowed to cool to room temperature before Chemlok® 205/220 adhesive was applied. Each plate was placed in a cavity mold with a sufficient amount of uncured neoprene 5109S rubber to provide the desired layer thickness. The mold was then placed in preheated platen press and brought up to vulcanizing temperature and pressure over a period of 5–10 min (315°F and 20 ksi, respectively). After curing at the specified temperature and pressure for 50 min, the mold was removed and allowed to cool to room temperature overnight.

Bond flaws were formed by coating the designated flaw area with a mold-release, Dow-Corning Type 33 silicone grease. The mold release was rubbed into the surface with a nylon burnishing tool. A continuous adhesive layer was formed across the flaw area. Flaw areas that continued to the edge of the specimen were sealed at the edge with RTV silicone sealer.

Instrumentation

A photograph of the LLW measurement system is shown in Figure A.1. The signal source is an Analogic Model 2020 Polynomial Waveform Synthesizer. It

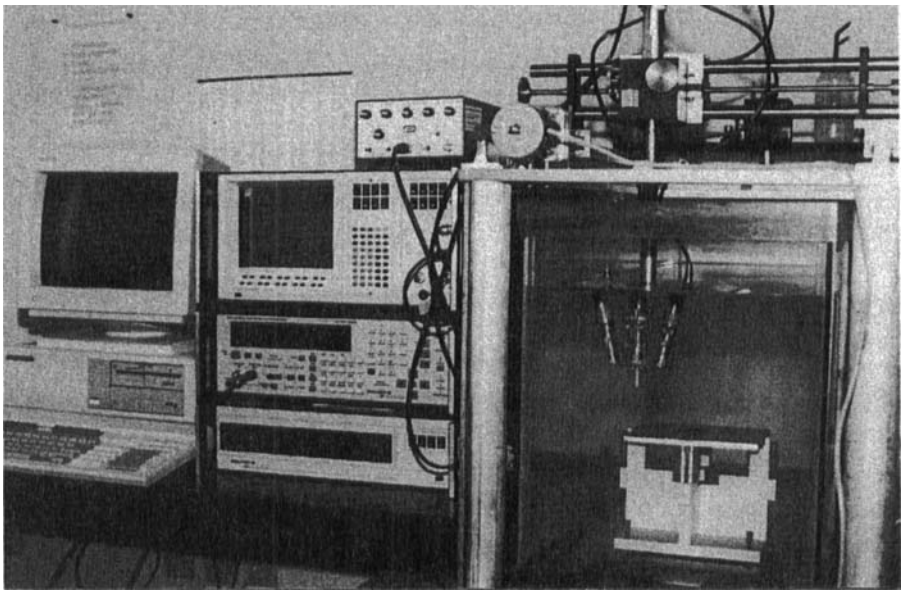

FIGURE A.1 Photograph of the leaky Lamb wave experimental set-up.

drives an ENI Model 240L RF Power Amplifier. The transducers are Harisonic immersion units resonant at 0.5, 1.0, 2.25, 5.0 or 7.5 MHz with element diameters of 0.25, 0.5 and 1 in. The measurements reported here were all made using 0.5 in. elements.

Waveform display, signal processing and analysis are done by the Analogic Model 6000 Waveform Analyzer. Scanning and data acquisiton control are done with the H-P 82315A Basic Controller. During data acquisition, the analog signal waveform and the scan line being generated are displayed on the CRT of the Model 6000.

The H-P 82315A controls two Compumotor stepper-motors that move the transducer carriage in the X and Y directions (vertical and rotational adjustments are performed manually). Scanning is done in the X direction with 128 sample points per scan line. With a scan length of 5 in. one measurement (sample point) is taken every 0.04 in. The carriage is then stepped 0.1 in. in the Y direction and another line is run. A complete scan consists of 51 lines (5 in. in the Y direction).

The controller starts and stops the signal processing and display functions of the Model 6000. Each scan line generated is copied to the H-P82315A and displayed on the CRT; display formats are discussed below. Hard copies can be prepared using the 6-Pen Plotter.

Set-up conditions

Specimen positioning is performed as follows. The specimen is placed in a holder which permits fine leveling adjustments along both the X and Y axes. The Panametrics Pulser-Receiver is used with a 7.5 MHz transducer (aligned with the axis of the supporting shaft for the LLW transducers) to measure transducer-specimen surface separation distance. Separation distance is measured near the mid-points of the edges of the specimen, normally 0.5 in. inboard. Leveling adjustments are made to align the exposed surface of the specimen as nearly parallel as practicable to the plane of the scanning transducers. In general, the specimens are not perfectly flat, that is, there are variations in planarity of up to a wavelength or so (in water) of the insonifying signal (8–10 μ in.). However, positioning is usually one-half wavelength or less at the edges.

The initialization signal is an approximately one-octave bandwidth, linear-frequency-modulated (LFM) chirp centered at 1.0 MHz, 2.25 MHz or 5.0 MHz. There is no theoretical basis at this time for selecting a particular frequency band, or operating frequency within a band. Several frequencies (modes) within a band are usually tested before selecting one to use. Candidate frequencies (modes) are tested by running single scan lines across the surface of the specimen, usually in an area with a known flaw, and evaluating signal and background characteristics. Single scan lines at several locations are often run before selecting a frequency (mode).

The scanning procedure begins with the transducers positioned well above the surface of the plate in the far field. At such location, the specularly reflected LFM echo dominates the received signal; LLWs are not detected. Reducing the transducer-surface separation (fixed transducer mounting geometry) until the

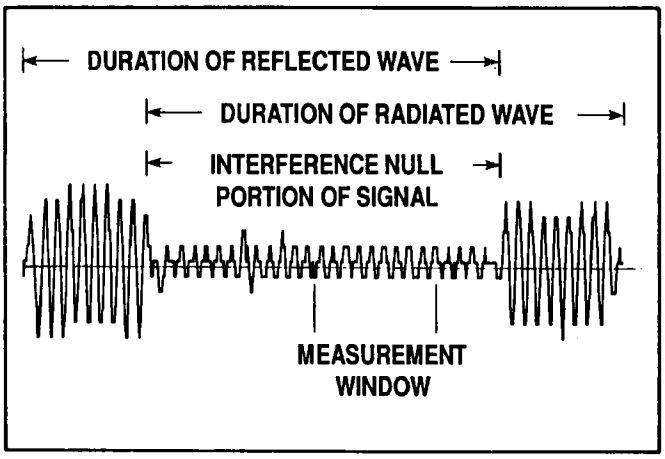

FIGURE A.2 Description of the null response due to interference between the specular wave and the leaky wave.

amplitude of the detected specularly reflected echo is reduced due to reaching the null induced by the Leaky plate wave. A Fast Fourier Transform of the received signal is computed to reveal the frequencies of the nulls that are associated with the excitation of Lamb wave modes. Next, the signal form is changed to a tone-burst at one of the null, or modal, frequencies, yielding a null signal at the receiving transducer. The latter signal form is illustrated in Figure A.2. The transducer-surface separation is then adjusted to minimize the amplitude within the null portion of the signal. Ordinarily, the transmit-receive plane is oriented normal to the scanning direction to maximize coverage of the scanned area. If a plate is anisotropic, with the grains oriented in a particular direction, then scattering of the internally propagating wave by the grains can significantly degrade the null signal. The magnitude of this scattering can be reduced by orienting the transmit-receive plane at various angles to the grain direction. This is done by rotating the transducers around the axis of the supporting shaft while monitoring the amplitude within the null portion of the received signal. The transducers are fixed at the orientation that yields the lowest amplitude. A scan line is then run. Generally, this procedure is followed for all modal frequencies tested.

Measurement procedures

The null signal, Figure A.2, is gated and the RMS level of the gated portion computed. This level is tracked as the transducers move across the surface of the specimen to generate a scan line. These operations are performed by the Model 6000 Waveform Analyzer. The measurement is not normalized.

Stored scans are displayed in two formats: (1) a simple waterfall or *pseudo* three-dimensional format wherein successive lines are offset slightly in both the X

and Y directions, and (2) a C-scan format, using either a gray-scale or colors to indicate signal amplitude. Typically, five amplitude ranges are used in the C-scan display. At this stage in the development of the LLW method, both formats are necessary. The waterfall format enables detecting small amplitude perturbations (including dips). Also, the waterfall display provides guidance for establishing the ranges of amplitudes for the C-scan to yield a meaningful display. Both display formats are illustrated in the present work.